# Cascaded Sapphire Fiber Bragg Gratings Inscribed by Femtosecond Laser for Molten Steel Studies

Dinesh Reddy Alla, Deva Prasad Neelakandan, Rex E. Gerald II, Laura Bartlett, Ronald J. O'Malley, Todd P. Sander, Jeffrey D. Smith, Jie Huang. *Senior*, *Member IEEE* 

Abstract --- This paper presents a distributed fiber optic hightemperature sensing system for steel industry applications. In recent years, optical sensors using sapphire fibers were investigated for harsh environment sensing. Sapphire optical fibers offer a high melting point of over 2,072 °C, good transparency in the telecommunication band, corrosion resistance, and immunity to electromagnetic interference. Cascaded fiber Bragg gratings (FBGs) were fabricated in a multimode sapphire optical fiber utilizing a femtosecond laser, The FBGs provided distributed sensing capability and were tested at ultra-high temperatures (1,800 °C). The FBG reflection spectrum was investigated by developing a multimode demodulation system, which aided in performing accurate (99.98 %) temperature measurements. The thermal stability of sapphire FBGs at 1600 °C for 22 hours was also demonstrated. Furthermore, distributed temperature sensing using multiple sapphire FBGs and their application in molten steel studies through temperature measurements are also reported. The aforementioned sensors can be used for continuous temperature monitoring in harsh environments such as in steel molds, refractory components, furnaces, turbine engines, and boilers.

Index Terms— Fiber Bragg gratings (FBGs), fiber sensors, sapphire optical fiber, femtosecond (fs) laser, molten steel, submerged entry nozzle (SEN).

# I. INTRODUCTION

APPROXIMATELY 88 million tons of steel were produced in the U.S. in 2016, with a weighted average energy intensity of approximately 18 MBTU/ton[1]. Small improvements in operating stability, efficiency, and product yield translate to substantial energy cost savings for the industry on an annual basis. The annual total energy expenditures in the U.S. steel industry exceed six billion dollars. A 10% enhancement of energy efficiency would lead to 600 million dollars in savings per year in the U.S. steel industry[2]. Production of 1 ton of crude steel generates about 1.9 tons of carbon dioxide. The improvement of production efficiency and the elimination of waste will also lead to a significant reduction in carbon dioxide emissions. Distributed temperature measurements at various molten steel processing stages will

lead to an increase in production efficiency and a reduction in energy requirements.

In steel manufacturing, several areas in the continuous casting process would benefit from distributed temperature measurement at steelmaking temperatures. One such area is the submerged entry nozzle (SEN), which is the refractory component that transfers the liquid steel from the tundish to the mold, protects the steel from air exposure, and directs the steel flow in a controlled manner in the mold. A distributed temperature sensor array placed within the SEN wall could be used for submergence control, SEN wear monitoring, monitoring of wave activity and flow asymmetry in the mold, and continuous steel temperature monitoring in the mold. Such measurements would enable improvements in quality, safety, and production efficiency in the continuous casting process. <sup>1</sup>

In recent years fiber optic sensors have proven to be valuable sensing systems with higher accuracy, high measurement resolution, and wide sensing range compared to thermocouples. One of the commercially available and commonly used fiberoptic sensors was the Fiber Bragg Gratings (FBGs)[3], [4]. Various applications of FBGs for measuring strain and temperature in industries were widely discussed[5], [6]. In recent years, the application of FBGs for temperature measurements in the steel industry has been extensively reported[7]-[10]. In 2013 Lieftucht et al, successfully developed a continuous caster mold monitoring system through temperature measurements using FBGs, known as a highdefinition mold (HD mold). Later, Wans et al, described the improvement in process stability and enhancement in product quality obtained by monitoring the heat transfer in an HD mold, which provided sufficient time for the operator to take actions necessary correct anomalous casting conditions. In 2018, Castiaux et al, reported an efficient way of installing FBGs in copper molds and evaluated their potential for thermal mapping of liquid steel and breakout detection of mold during steel casting.

Conventional FBGs are developed through an ultraviolet (UV) laser-based phase mask method, where the optical fiber undergoes type-I refractive index modulation. However, the type-I index modulated FBGs typically have low operating

Dinesh Reddy Alla, Rex E. Gerald II, and Jie Huang are with the Department of Electrical and Computer Engineering, Missouri University of Science and Technology, Rolla, MO 65409 USA. (Corresponding author: Jie Huang, jieh@mst.edu). Deva Prasad Neelakandan, Laura Bartlett, Todd P. Sander, Jeffrey D. Smith, and Ronald J. O'Malley are with the Department of Material Science and Engineering, Missouri University of Science and Technology, Rolla, MO 65409 USA.

<sup>&</sup>lt;sup>1</sup> This paragraph of the first footnote will contain the date on which you submitted your paper for review. This material is based upon work supported by the Peaslee Steel Manufacturing Research Center (PSMRC) and the U.S. Department of Energy's Office of Energy Efficiency and Renewable Energy (EERE) under the Advanced Manufacturing Office (AMO) Award Number DE-EE0009119. The views expressed herein do not necessarily represent the views of the U.S. Department of Energy or the United States Government.

temperatures (< 450 °C). Another solution was to use a femtosecond (fs) laser to fabricate FBGs through a point-bypoint method. The fs laser creates type-II refractive index modulation along the optical fiber and can withstand extremely harsh environments and that can measure high temperatures (~1,800 °C) [11]–[16]. In the last decade, Mihailov et al, reported various applications of fs-laser fabricated FBGs in harsh and extreme environmental conditions. The fs laser fabricated single-mode silica FBGs have provided efficient and accurate sensing means for temperatures < 1,200 °C but for temperatures beyond 1,200 °C, sapphire optical fiber-basedsensors would provide a viable option for accurate temperature sensing. This was due to their advantages of high mechanical strength, high melting point (~ 2,072 °C), corrosion resistance, chemical stability, and immunity from electromagnetic interference[17], [18]. In 2021 Wang et al, discussed sapphire optical fiber-based ultra-high temperature sensing systems based on FBGs, interferometry, Raman scattering, and sapphire thermometry principles. Unlike silica-based optical fibers, the sapphire fibers are fabricated in the shape of semi-cylindrical rods without a layer of cladding, and with commercially available fiber diameters, the beam propagation in the optical is highly multimodal at the near-infrared telecommunication bands.

Sapphire optical fiber thermometry was a single-point temperature sensing system that uses thermal radiation from a sapphire optical fiber for temperature sensing [17], [19]–[21]. In 2021, Qian et al, successfully demonstrated a nanorod alumina coated sapphire fiber-based optical fiber thermometer for temperature analysis in molten steel. However, the sensing principle was based on the intensity analysis of thermal radiation spectra, which can be affected by ambient light coupling and variations in fiber position. To overcome these issues, a convolution neural network algorithm was developed and trained for temperature classification from the thermal radiation spectra[21].

The fs-laser inscribed sapphire FBGs are reported to be stable, efficient, and effective for harsh environments and ultrameasurements[22]–[24]. temperature Habisreuther et al, reported an fs-laser fabricated air-clad sapphire FBG for temperature measurements in the range of 1,900 °C along with FBG multiplexing for distributed sensing. The fs laser fabricated sapphire FBGs based on phase masks for temperature and strain sensing were previously discussed [15], [25], [26]. In 2009 Busch et al, reported the fs-laser phase mask fabricated sapphire FBG for temperature measurements in the range of 1,750 °C along with a long-term test with temperatures cycling between 1,200 °C and 500 °C for 120 hours. The commercially available sapphire optical fibers are highly multimodal, hence the fs laser line-by-line scanning method was commonly applied for FBG fabrication, which resulted in higher reflectivity [27]–[30] over the point-by-point fabrication method[31], [32]. In 2019 Xu et al, investigated fs laser-based line-by-line fabricated FBGs reflectivity and SNR change compared to FBGs fabricated at different layers and layer spacings within the diameter of the fiber. The line-by-linebased fabrication method has resulted in sapphire FBGs with greater reflectivity.

Despite the highly reflective sapphire FBGs, most of the reported sapphire FBG spectra exhibit poor signal-to-noise ratio, distorted peaks, low fringe visibility, and broad linewidth. These issues are mainly due to the highly multi-modal interference of the air-cladded sapphire optical fibers. Efforts have been made to address these issues including the investigation of proper cladding materials to minimize the number of modes [33], the fabrication of a near-single mode sapphire optical fiber [32], and the use of an ultra-long lead-in optical multimode fiber to reduce the multimodalinterference[22], [26], [30], [34]. The cladded sapphire optical fibers have shown reduced numerical apertures but most of the cladding materials can only withstand up to 1,400 °C due to the mismatch in the thermal expansion coefficients of the coating and sapphire materials. The near-single mode sapphire optical fiber can be a good solution but with a drastically reduced diameter that may degrade the mechanical strength of the fiber. An ultra-long lead-in optical multimode fiber can reduce the multimodal interference to some extent but still cannot drastically minimize it. Moreover, rigorous packaging of the lead-in fiber was also required. In summary, there remains a strong need for the development of sapphire FBGs exhibiting high-quality reflection spectra and a novel interrogation unit to eliminate multimodal interference.

In this paper, we report the fs laser-based sapphire FBG fabrication through a line-by-line scanning method, which results in high reflectivity, good signal-to-noise ratio (SNR), a low full width at half maximum (FWHM), and a thermal stability of long duration. A novel mode scrambler method was also included in the interrogation unit to drastically minimize the multimode interference of sapphire optical fiber. The FBG was tested at temperatures of up to 1,800 °C and, for the first time to our knowledge, the fiber was employed for measurements in molten steel by embedding the fiber into an alumina-graphite SEN refractory to monitor temperature during the direct immersion of the refractory into molten steel.

# II. EXPERIMENT

A femtosecond laser (Spirit One, Spectra-Physics) with pulse duration <400 fs at a reputation rate of 200 kHz was used for sapphire FBG inscription following a line-by-line laser scanning method. The laser system was integrated with an efficient second harmonic generation (SHG) module, which enabled switching the laser central wavelength between 520 nm and 1040 nm. The laser was customized to work at 520 nm at a 5 kHz repetition rate and 500 nJ/pulse. The custom-built fslaser microfabrication system contains an fs-laser and an automized workstation (femtoFBG, Newport Corporation). The translation stage assembly (Newport, XMS100) included in the workstation provided a 3-dimensional displacement accuracy of 0.05 µm across the x-axis and <1nm resolution across the y and z-axes. The average laser power was controlled by a halfwave plate and Glan-laser polarizer, built inside of femtoFBG workstation. The fs-laser pulses were reflected through a

dichroic mirror and centered into the fiber using a 40X nonimmersion objective lens. The fiber alignment and FBG fabrication process were observed in real-time using a CMOS camera. The microfabrication system was controlled by a computer through a custom-built graphical user interface (GUI). The FBGs were fabricated by following the phasematching condition as shown in eq (1).

$$m\lambda_{Bragg} = 2n_{eff}\Lambda_g \tag{1}$$

Where m is the FBG order,  $\lambda_{Bragg}$  is Bragg wavelength,  $n_{eff}$  is the effective refractive index and  $\Lambda_g$  is the grating period of the FBG. The effective refractive index of sapphire is 1.745 at 1,550 nm. In- order to make strong FBG reflectors, a high pulse repetition rate and high laser intensity were applied, which led to a larger spot size, resulting in selecting a larger grating period. Higher-order FBGs were fabricated to facilitate the laser spot size, and a grating period of 2.19  $\mu$ m gave 5<sup>th</sup>-order FBGs with a Bragg wavelength of 1,603.2 nm.

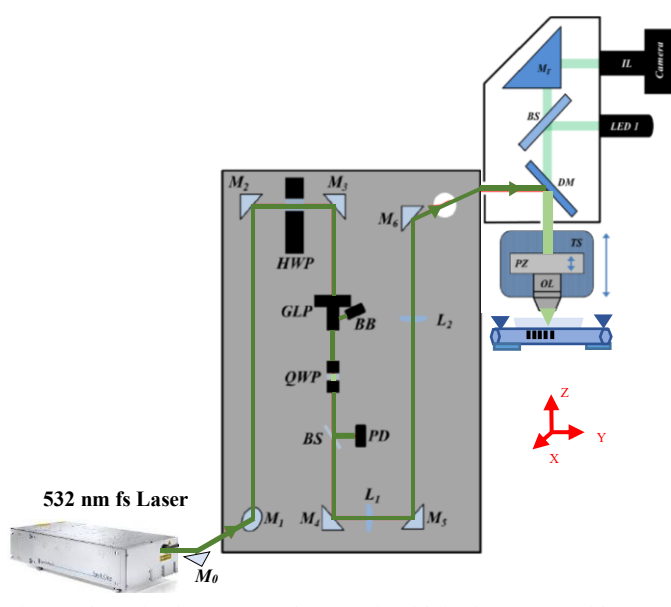


Fig. 1. Schematic of Femtosecond Laser Microfabrication System with M<sub>0</sub>-M<sub>6</sub>: mirrors, HWP: half-wave plate, GLP: Glan-laser polarizer, BB: beam block, QWP: quarter-wave plate, BS: beam sampler, PD: photodiode, L<sub>1</sub>-L<sub>2</sub>: lens, DM: dichroic mirror, MT: turning mirror, IL: imaging lens system, OL: objective lens, PZ: piezo stage, TS: translational stage

Sapphire FBGs were fabricated in a 125  $\mu$ m diameter airclad, 30 cm long sapphire fiber (MicroMaterials Inc, Tampa, FL, USA). The fabrication process was observed through a CMOS camera. To fabricate FBGs with 90  $\mu$ m length, the origin (0,0,0) of the fabrication profile was set 12.5  $\mu$ m away from the fiber boundary and into the fiber. The laser shutter opens, and the 3D stage moves 90  $\mu$ m along the negative x-axis direction, drawing a 90  $\mu$ m line in the sapphire fiber. The laser shutter closes, and the stage moves along the y- axis direction to the point (0, 2.29  $\mu$ m,0). This process was repeated until the total moving distance along the positive y-axis reaches 7 mm, to the point (90  $\mu$ m,7000  $\mu$ m,0). The moving speed of the stage along the x-axis was 100  $\mu$ m/s and along the y-axis was 1000  $\mu$ m/s. The sapphire FBG was excited by connecting it to a

 $105/125~\mu m$  multimode silica fiber using a mechanical splicer through a 50:50 multimode coupler. The signal from a high power, broadband supercontinuum laser source (400-2,000~m) was launched into the multimode scrambler (MMS-201) and the output of the multimode scrambler was connected to the multimode coupler. The Optical Spectrum Analyzer (OSA) collects the reflections from FBGs. The mode scrambler effectively randomizes the light from the laser source over time at a frequency of 150 kHz so that the light distribution at the output was uniform and stationary, which helped reduce the multimodal interferences.

For the molten steel immersion test, a test frame with a motorized immersion and retraction mechanism was used to position the sample in the molten steel bath. A 200 lb. induction furnace capable of melting and holding steel at temperatures exceeding 1,600°C (3,000°F) for 30 minutes was used. The sapphire fiber was housed in a cylindrical sample tube made of alumina-graphite SEN refractory to measure the temperature gradient along the length of the sample. An S-type thermocouple was used for a reference temperature measurement for comparison. Fig. 2(b) shows the alumina graphite rod which was 6" in height and 2" in diameter. A 0.5" diameter 5" deep hole was drilled to house the reference S-type thermocouple and the 18" long sapphire fiber with three inscribed FBGs.

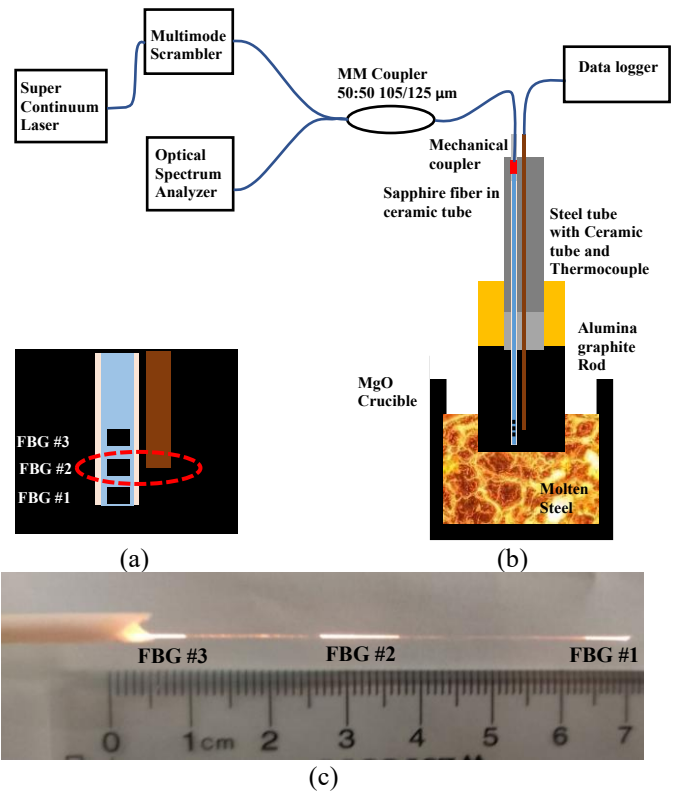


Fig. 2. First demonstration of Sapphire FBGs in molten steel immersion test. (a) Sapphire FBG positions are shown with respect to a thermocouple. (b) Schematic diagram of FBG reflection spectrum measurement setup. (c) Image of Sapphire fiber showing FBG sections illuminated by the supercontinuum laser

The sapphire fiber was sheathed in an alumina tube of 0.219" OD x 0.156" ID to provide mechanical strength. A stainless-steel tube was connected to the ceramic tube using a high-

temperature adhesive (JB Weld, 1,000 °C) and was used to sheath the fiber and splice point up to the interrogation system. The wires of the S-type thermocouple were sheathed in a double-bore ceramic tube of 0. 125" OD x 0.04" ID. The fiber with FBGs was immersed into molten steel such that two FBGs were below the molten steel and one FBG was above the melt. A schematic of this arrangement is shown in Fig. 2 (a). Each FBG was 7 mm (0.28") long, across the longitudinal axis of the sapphire fiber. The spacing between the end face and FBG#1 was 12.7mm. The space between FBG #1 and FBG #2 was 25 mm. The space between FBG #2 and FBG #3 was 15 mm. The thermocouple tip was placed next to FBG #2. The placements of the FBGs and thermocouple tip were carefully aligned to measure a good temperature comparison between the thermocouple and FBG #2.

### III. RESULTS AND DISCUSSION

FBGs were fabricated within the sapphire fiber with 90  $\mu$ m line lengths, grating periods of 2.19  $\mu$ m, and lengths of 7 mm. Figs. 3 (a) and (b) show microscope images of example gratings. The gratings are 90  $\mu$ m in length and 60  $\mu$ m in width. The reflection spectrum contains a peak with an SNR of 6.54 dB and an FWHM of 5.66 nm. The multimode scrambler, inserted into the sapphire fiber FBG light excitation path, helped provide uniform light distribution through the entire cross-section of the fiber, which led to a more stable and uniform reflection spectrum.

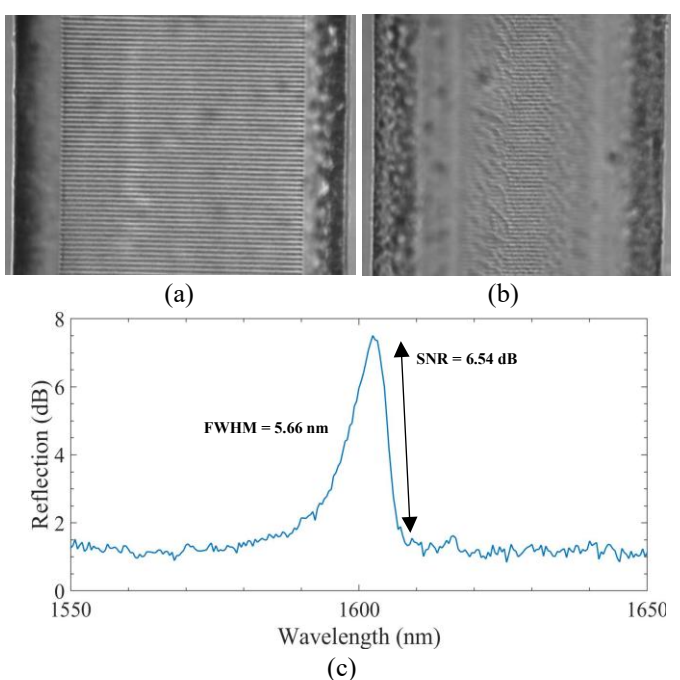


Fig. 3. Microscope images of a sapphire FBG (a) Top View. (b) Side View and (c) Sapphire FBG reflection spectrum.

Additionally, two new FBGs were fabricated on a 30 cm long fiber with fiber length sufficient for installation in a heating furnace for observing the Bragg wavelength shift to temperature changes. Fig. 4 (a) shows the reflection spectrum at room temperature (24 °C). The sapphire fiber with the FBG end was placed into a custom-built high-temperature induction

furnace. The light scattered by the FBGs was used to fix the FBG position at the center of the furnace. The spectral response of the sapphire FBGs with varying temperatures up to 1,800 °C is shown in Fig. 4 (b). An increase in Bragg wavelength ( $\lambda_{Bragg}$ ) with increasing temperature is expected and confirmed. The induction furnace temperature was monitored using an S-type thermocouple with a measurement range of 2,000 °C.

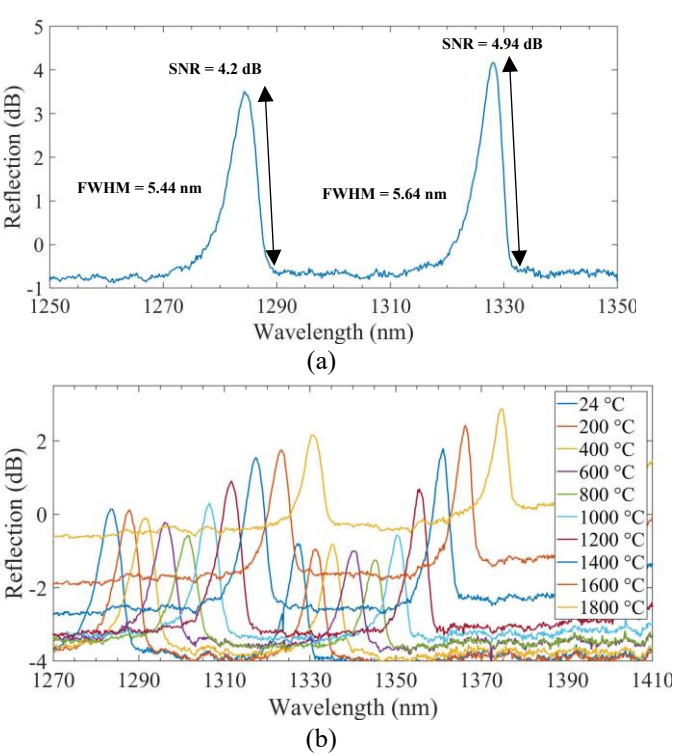


Fig. 4. Reflection spectra of two sapphire FBGs fabricated for high-temperature induction furnace tests. (a) Reflection spectra at room temperature (24 °C), (b) The sapphire FBG  $\lambda_{Bragg}$  increases by 7.2 nm for temperature increments of 200 °C up to 1800 °C.

The fs-laser written gratings survived temperature exposure of 1,800 °C for 45 minutes. For temperatures above 1,400 °C the SNR of the reflection peak diminished due to strong background light generated from the thermal radiation of the sapphire optical fiber. The use of a multimode scrambler helped in obtaining stable and accurate reflection spectra for various temperatures. Molten steel temperatures are typically around 1,600 °C, hence the spectrum shifts of the FBGs for heating and cooling cycles up to 1,600 °C were observed, as shown in Fig. 5, and are of interest for additional high-temperature experiments.

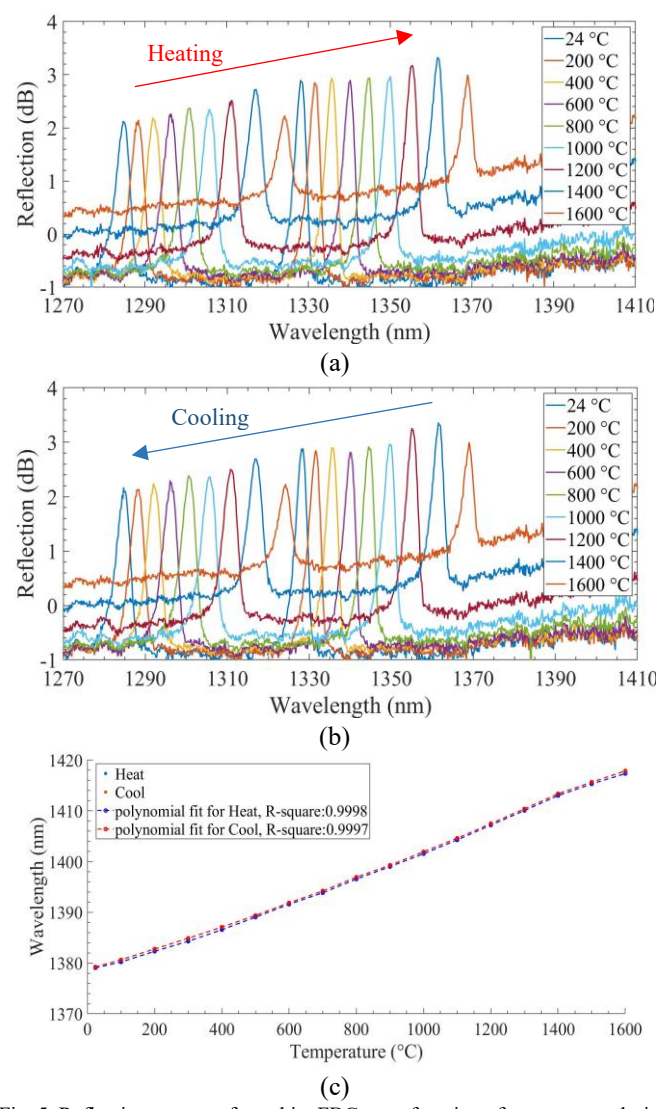


Fig. 5. Reflection spectra of sapphire FBGs as a function of temperature during (a) heating cycle, (b) cooling cycle, (c) Polynomial curve fit for sapphire FBG Bragg wavelength ( $\lambda_{Bragg}$ ) versus temperature data for a heating and cooling cycle.

Fig. 5 (c) shows the wavelength change with increasing temperature and a polynomial curve fit with 99.98 % accuracy for the heat cycle and 99.97 % accuracy for the cool cycle. The plot of wavelength change with rising temperature shows a sensitivity of 33.55 pm/°C. A third-order polynomial transfer function was developed for efficient wavelength to temperature conversion up to 1,600 °C. The polynomial transfer function is given by

$$\lambda_{Bragg} = 1603.2 + 0.0166T + 10^{-6}T^2 - 3.000 * 10^9T^3$$
 (2)

Furthermore, to perform a longer duration thermal stability analysis of the sapphire FBGs, the sapphire fiber with FBGs was inserted into a ceramic furnace (Criferon Model. SiC based). A 4°C/min temperature ramp up was used to reach 1,600°C and FBG reflection spectra were recorded for 22 hours to test FBG stability. The furnace temperature was controlled using an 80%-20% platinum-rhodium thermocouple and a second S-type thermocouple was placed close to one of the

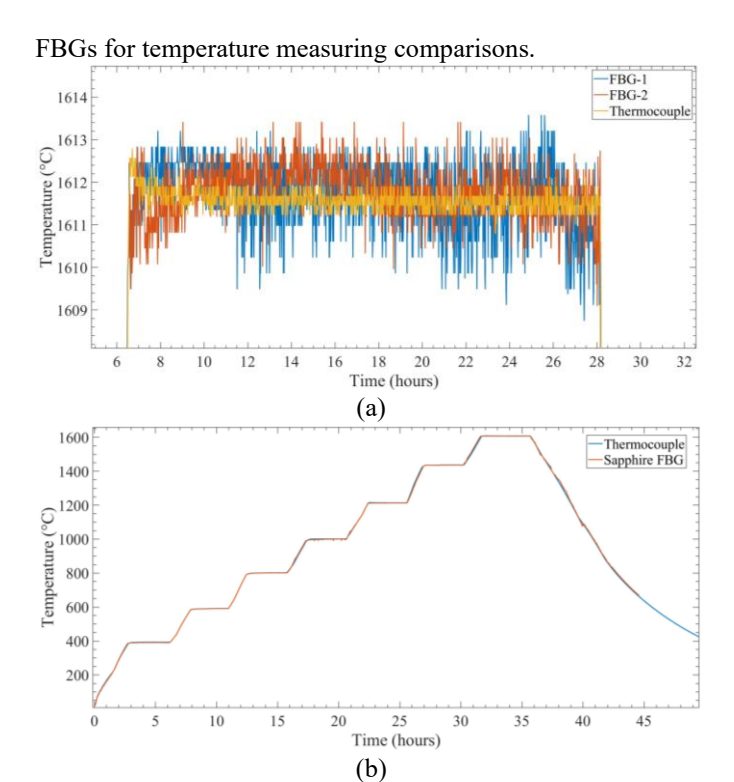
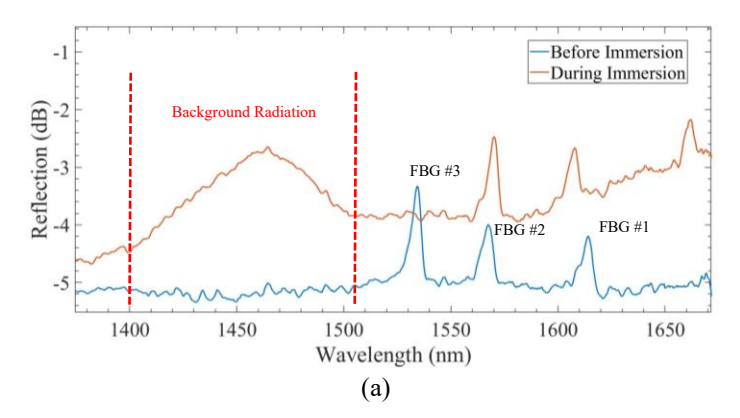


Fig. 6. Comparison of temperatures measured by sapphire FBGs and a thermocouple (S-type). (a) Temperature stability of +/- 2 °C for 22 hours, (b) Various rise and hold temperatures in a heat cycle.

Fig 6 (a) shows the comparison of temperatures measured by thermocouple and a sapphire FBG at 1,612°C for 22 hours; less than a +/-2°C thermal drift was observed for sapphire FBG measured temperature. Fig. 6 (b) shows a good match of temperature measured by the sapphire FBG and an S-type thermocouple for various hold and rise temperatures performed in a single heat cycle demonstrating the accuracy of eq (2).

For the molten steel immersion experiment, a single sapphire fiber with three FBGs was employed in the immersion setup shown in Fig. 2(b). Reflection spectra were recorded for 30 minutes during the immersion experiment. The reflection spectra of the FBGs before (at room temperature) and during immersion (at liquid steel temperature) are shown in Fig. 7 (a). The background high-temperature thermal radiation peak can be observed in the 1,400-1,500 nm wavelength range along with the Bragg wavelength shifts of the inscribed FBGs. The comparisons of temperatures measured by the #2 sapphire FBG and the S-type thermocouple are shown in Fig. 7(b).



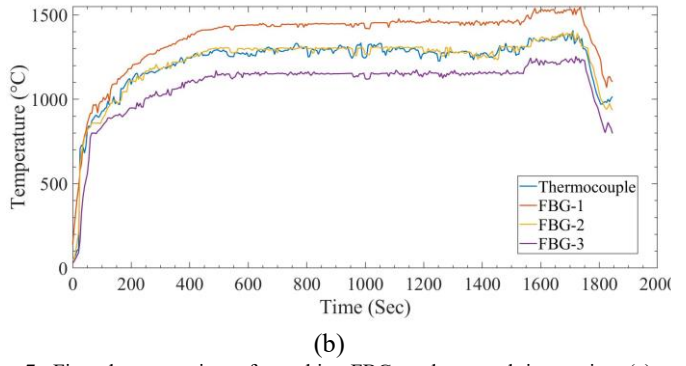


Fig. 7. First demonstration of sapphire FBG molten steel immersion (a) Reflection spectra of sapphire FBGs before and during immersion. (b) Comparison of temperatures measured by the sapphire FBGs and the thermocouple (S-type).

Fig 7(b) shows a close match between temperatures measured using FBG #2 and the nearby thermocouple. The sapphire fiber survived immersion into molten steel and successfully monitored temperatures along the alumina graphite sample tube for 30 minutes. The third-order polynomial transfer function developed above (eq. 2) facilitates accurate temperature measurements and the ceramic tube protects the sapphire fiber from contamination, making the sensors reusable.

### IV. CONCLUSION

Using a femtosecond laser, FBGs were fabricated in a sapphire optical fiber through a line-by-line scanning method, which yielded FBG reflection spectra with high SNR (6.54 dB) and low FWHM (5.66 nm). The application of a mode scrambler (MMS-201) in an FBG demodulation system helped in obtaining stable and accurate reflection spectra. The narrow Bragg wavelength peak allowed for efficient and accurate temperature measurements of greater than 1,600 °C. The thermal stability analysis of sapphire FBGs demonstrated temperature measurements with a 0.125 % error (+/- 2°C thermal drift). The first demonstration of sapphire FBGs for molten steel immersion experiment using alumina-graphite SEN refractory for successful temperature monitoring suggests that sapphire FBG sensors will be ideal for use in submerged entry nozzles and refractory linings. The efficiency and accuracy of sapphire FBG sensors over conventional thermocouples will lead to increases in productivity, reduction of power consumption, and a smaller carbon footprint for the steel industry.

# REFERENCES

- [1] "Energy Intensity of Major Steelmaking Units", AISI Steel Works Site, March 2017.
- [2] https://www.automation.com/en-us/articles/december-2020/impacting-energy-through-smart-manufacturing. Accessed on October 23, 2021.
- [3] R. Kashyap, "Fiber Bragg Gratings," *Fiber Bragg Gratings*, vol. 4309, no. March 1997, 2010, doi: 10.1016/C2009-0-16830-7.
- [4] J. Chen, B. Liu, and H. Zhang, "Review of fiber Bragg grating sensor technology," *Frontiers of*

- *Optoelectronics in China*, vol. 4, no. 2, pp. 204–212, 2011, doi: 10.1007/s12200-011-0130-4.
- [5] D. Kinet, P. Mégret, K. W. Goossen, L. Qiu, D. Heider, and C. Caucheteur, "Fiber Bragg grating sensors toward structural health monitoring in composite materials: Challenges and solutions," Sensors (Switzerland), vol. 14, no. 4, pp. 7394–7419, 2014, doi: 10.3390/s140407394.
  - X. Qiao, Z. Shao, W. Bao, and Q. Rong, "Fiber bragg grating sensors for the oil industry," *Sensors* (*Switzerland*), vol. 17, no. 3, 2017, doi: 10.3390/s17030429.

[6]

- [7] D. Lieftucht, M. Reifferscheid, T. Schramm, A. Krasilnikov, and D. Kirsch, "HD mold A new fiber-optical-based mold monitoring system," *Iron and Steel Technology*, vol. 10, no. 12, pp. 87–95, 2013.
- [8] J. Wans, D. Lieftucht, C. Geerkens, M. Arzberger, and M. Reifferscheid, "HD mold - Caster assistance system to increase product quality," AISTech - Iron and Steel Technology Conference Proceedings, vol. 2, no. May 2013, pp. 1385–1391, 2013.
- [9] E. Castiaux and R. Robert, "Use of FBG optical fibers in CC mould for Bo detection and thermal exchange supervision first trial in a broadface on a stainless steel slab caster," ICS 2018 7th International Congress on Science and Technology of Steelmaking: The Challenge of Industry 4.0, no. June, 2018.
- [10] T. Spierings, A. Kamperman, H. Hengeveld, J. Kromhout, and E. Dekker, "Development and application of fiber bragg gratings for slab casting," AISTech - Iron and Steel Technology Conference Proceedings, vol. 2, no. May, pp. 1655–1663, 2017.
- [11] J. He, B. Xu, X. Xu, C. Liao, and Y. Wang, "Review of Femtosecond-Laser-Inscribed Fiber Bragg Gratings: Fabrication Technologies and Sensing Applications," *Photonic Sensors*, vol. 11, no. 2, pp. 203–226, 2021, doi: 10.1007/s13320-021-0629-2.
- [12] S. J. Mihailov, "Fiber bragg grating sensors for harsh environments," *Sensors*, vol. 12, no. 2. pp. 1898–1918, Feb. 2012. doi: 10.3390/s120201898.
- [13] S. J. Mihailov *et al.*, "Extreme environment sensing using femtosecond laser-inscribed fiber bragg gratings," *Sensors (Switzerland)*, vol. 17, no. 12, 2017, doi: 10.3390/s17122909.
- [14] C. R. Liao and D. N. Wang, "Review of femtosecond laser fabricated fiber Bragg gratings for high temperature sensing," *Photonic Sensors*, vol. 3, no. 2, pp. 97–101, Jun. 2013, doi: 10.1007/s13320-012-0060-9.
- [15] S. J. Mihailov, D. Grobnic, C. W. Smelser, P. Lu, R. B. Walker, and H. Ding, "Bragg grating inscription in various optical fibers with femtosecond infrared lasers and a phase mask," 2011.
- [16] C. Zhu, D. Alla, and J. Huang, "High-temperature stable FBGs fabricated by a point-by-point femtosecond laser inscription for multi-parameter sensing," *OSA Continuum*, vol. 4, no. 2, p. 355, Feb. 2021, doi: 10.1364/osac.415685.
- [17] B. Wang, Y. Niu, X. Qin, Y. Yin, and M. Ding, "Review of high temperature measurement technology

- based on sapphire optical fiber," *Measurement: Journal of the International Measurement Confederation*, vol. 184, 2021, doi: 10.1016/j.measurement.2021.109868.
- [18] C. Zhu, R. E. Gerald, and J. Huang, "Progress Toward Sapphire Optical Fiber Sensors for High-Temperature Applications," *IEEE Transactions on Instrumentation and Measurement*, vol. 69, no. 11, pp. 8639–8655, 2020, doi: 10.1109/TIM.2020.3024462.
- [19] G. van Eden *et al.*, "Measurement Science and Technology Enhancement on densification and crystallization of conducting La 0.7 Sr 0.3 VO 3 perovskite anode derived from hydrothermal process," 2001. [Online]. Available: www.iop.org/Journals/mt
- [20] Y. B. Yu and W. K. Chow, "Review on an Advanced High-Temperature Measurement Technology: The Optical Fiber Thermometry," *Journal of Thermodynamics*, vol. 2009, pp. 1–11, 2009, doi: 10.1155/2009/823482.
- [21] J. Qian *et al.*, "Machine learning-assited optical thermometer for continuous temperature analysis inside molten metal," *Sensors and Actuators, A: Physical*, vol. 322, May 2021, doi: 10.1016/j.sna.2021.112626.
- [22] T. Habisreuther, T. Elsmann, Z. Pan, A. Graf, R. Willsch, and M. A. Schmidt, "Sapphire fiber Bragg gratings for high temperature and dynamic temperature diagnostics," *Applied Thermal Engineering*, vol. 91, pp. 860–865, Dec. 2015, doi: 10.1016/j.applthermaleng.2015.08.096.
- [23] S. Yang, D. Homa, G. Pickrell, and A. Wang, "Fiber Bragg grating fabricated in micro-single-crystal sapphire fiber," *Optics Letters*, vol. 43, no. 1, p. 62, Jan. 2018, doi: 10.1364/ol.43.000062.
- [24] C. Hill *et al.*, "Single mode air-clad single crystal sapphire optical fiber," *Applied Sciences* (*Switzerland*), vol. 7, no. 5, 2017, doi: 10.3390/app7050473.
- [25] M. Busch, W. Ecke, I. Latka, D. Fischer, R. Willsch, and H. Bartelt, "Inscription and characterization of Bragg gratings in single-crystal sapphire optical fibres for high-temperature sensor applications," *Measurement Science and Technology*, vol. 20, no. 11, 2009, doi: 10.1088/0957-0233/20/11/115301.
- [26] T. Elsmann *et al.*, "High temperature sensing with fiber Bragg gratings in sapphire-derived all-glass optical fibers," *Optics Express*, vol. 22, no. 22, p. 26825, Nov. 2014, doi: 10.1364/oe.22.026825.
- [27] X. Xu, J. He, C. Liao, and Y. Wang, "Multi-layer, offset-coupled sapphire fiber Bragg gratings for high-temperature measurements," *Optics Letters*, vol. 44, no. 17, p. 4211, Sep. 2019, doi: 10.1364/ol.44.004211.
- [28] X. Xu *et al.*, "Sapphire fiber Bragg gratings inscribed with a femtosecond laser line-by-line scanning technique," *Optics Letters*, vol. 43, no. 19, p. 4562, Oct. 2018, doi: 10.1364/ol.43.004562.
- [29] D. Grobnic, S. J. Mihailov, C. W. Smelser, and H. Ding, "Sapphire fiber bragg grating sensor made using femtosecond laser radiation for ultrahigh temperature applications," *IEEE Photonics Technology Letters*,

- vol. 16, no. 11, pp. 2505–2507, Nov. 2004, doi: 10.1109/LPT.2004.834920.
- [30] Q. Guo *et al.*, "Femtosecond laser inscribed sapphire fiber bragg grating for high temperature and strain sensing," *IEEE Transactions on Nanotechnology*, vol. 18, pp. 208–211, 2019, doi: 10.1109/TNANO.2018.2888536.
- [31] S. Yang *et al.*, "Application of sapphire-fiber-bragg-grating-based multi-point temperature sensor in boilers at a commercial power plant," *Sensors* (*Switzerland*), vol. 19, no. 14, Jul. 2019, doi: 10.3390/s19143211.
- [32] S. Yang, D. Hu, and A. Wang, "Point-by-point fabrication and characterization of sapphire fiber Bragg gratings," *Optics Letters*, vol. 42, no. 20, p. 4219, Oct. 2017, doi: 10.1364/ol.42.004219.
- [33] H. Chen, M. Buric, P. R. Ohodnicki, J. Nakano, B. Liu, and B. T. Chorpening, "Review and perspective: Sapphire optical fiber cladding development for harsh environment sensing," *Applied Physics Reviews*, vol. 5, no. 1, 2018, doi: 10.1063/1.5010184.
- [34] S. J. Mihailov, D. Grobnic, and C. W. Smelser, "Hightemperature multiparameter sensor based on sapphire fiber Bragg gratings," 2010.